Supplementary Materials for

From rain to radiance - Dominant climate drivers of tropical carbon flux interannual variability depend on local hydroclimate

Shuang Ma, Junjie Liu@ *et al.*

*Corresponding author. Email: junjie.liu@jpl.nasa.gov

This file includes:

Text S1
Figs. S1 to S18
Tables S1

S1. Evaluation of CARDAMOM simulations of seasonal and interannual carbon and water variabilities.

As in any other Bayesian approaches, CARDMOM optimizes model states and parameters by minimizing the differences between model simulated quantities and assimilated observations, given their respective uncertainties. The optimization process balances the uncertainties from multiple observation sources to reach an optimal estimation, thus the fitting to the observations may vary depending on the relative uncertainties of each variable. CARDAMOM generates an ensemble of estimates to represent uncertainties of the posterior quantities. Figures S1-S4 show heatmaps of modeled GPP, NBE, TWS, and ABGB compared to assimilated observations over six tropical regions. Each point represents a monthly value at one of the 4º (latitude) x 5º (longitude) over the respective region. Figure S5-S7 show the comparison of monthly CARDAMOM median values and the assimilated observations. Figures S1-S4 show that the fittings to observations vary among variables. The fitting to GPP and ABGB by CARDAMOM are much better than the fitting to NBE and TWS. The correlations for GPP and ABGB exceed 0.9 across all regions. The correlation for NBE is greater than 0.47, while TWS shows correlations above 0.6 in most regions, except over Africa, where CARDAMOM exhibits a decreasing trend. However, the correlations between model simulations and observations are all statistically significant at the 99% confidence level ($p<0.01$) (Figure S5-S7). Because of the constraint on carbon and water quantities, CARDAMOM allows us to investigate the coupling between carbon and water coupling.

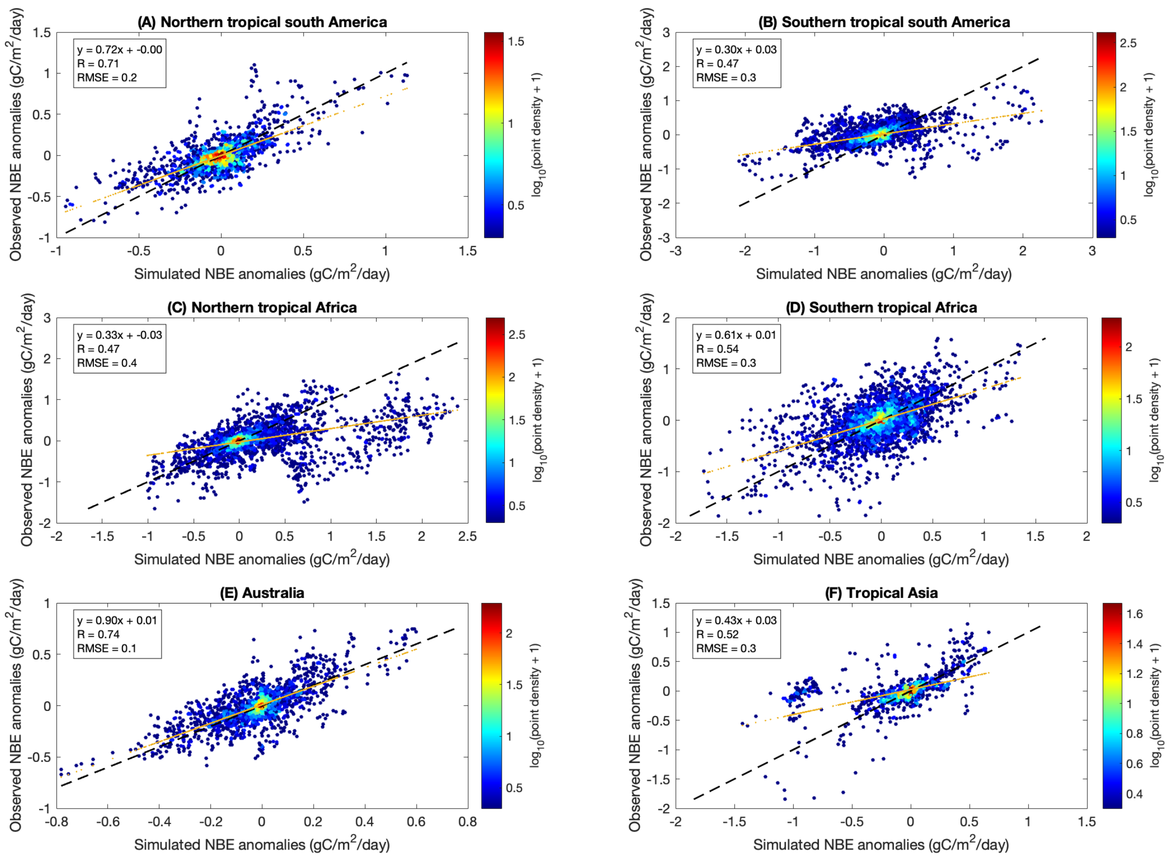

Figure S1 Heatmap of modeled five-month running mean of Net Biosphere Exchange (NBE) anomaly compared to observations at monthly temporal resolution (2010-2018) at pixel levels (4º (latitude) x 5º (longitude)). The pantropic region was grouped into Asia (AS), Australia (AU), Northern tropical Africa (NAF) (north of Equator), Southern tropical Africa (SAF) (south of Equator), Northern hemisphere South America (NSAM), and Southern hemisphere South America (SSAM). The R values, root mean square values, and linear fitting are labeled in each subplot. Unit: gC/m^2/day.

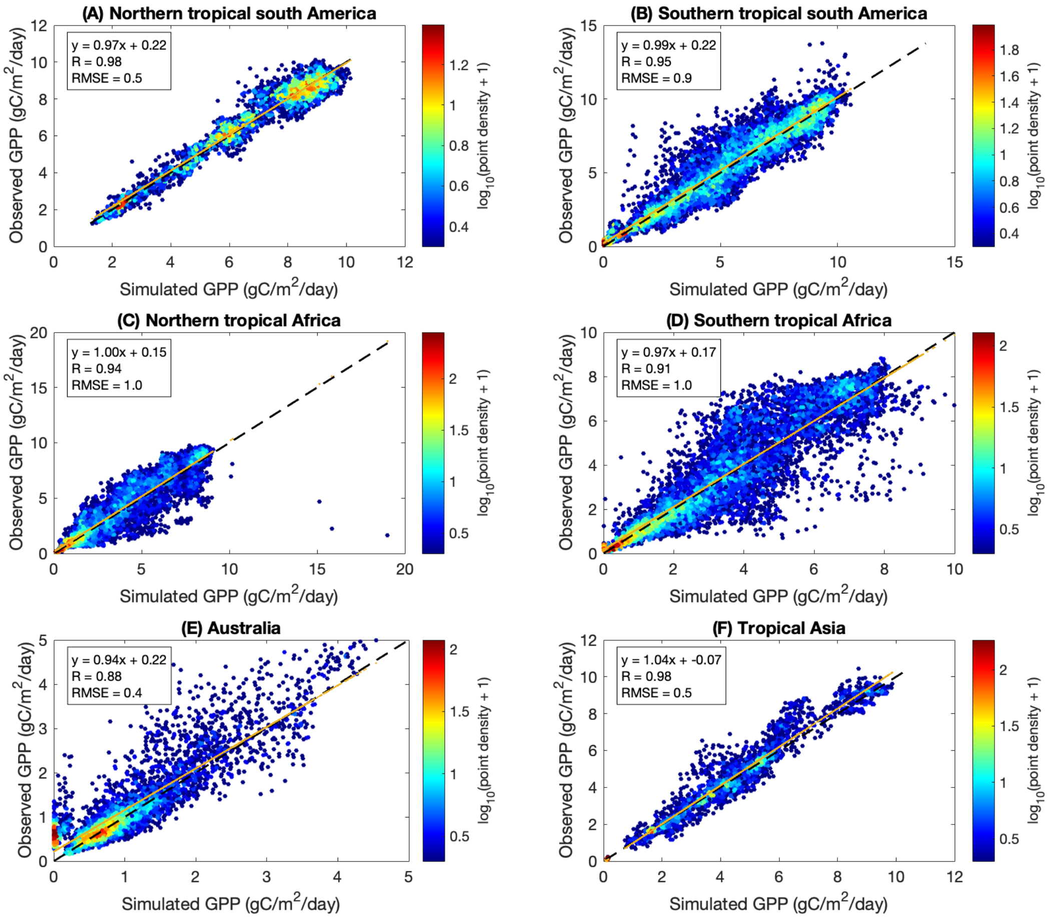

Figure S2 Heatmap of modeled gross primary production (GPP) compared to observations at monthly temporal resolution (2001-2021) at pixel levels (4º (latitude) x 5º (longitude)). The pantropic region was grouped into Asia (AS), Australia (AU), Northern tropical Africa (NAF) (north of Equator), Southern tropical Africa (SAF) (south of Equator), Northern hemisphere South America (NSAM), and Southern hemisphere South America (SSAM). The R values, root mean square values, and linear fitting are labeled in each subplot. Unit: $gC/m^2/day$.

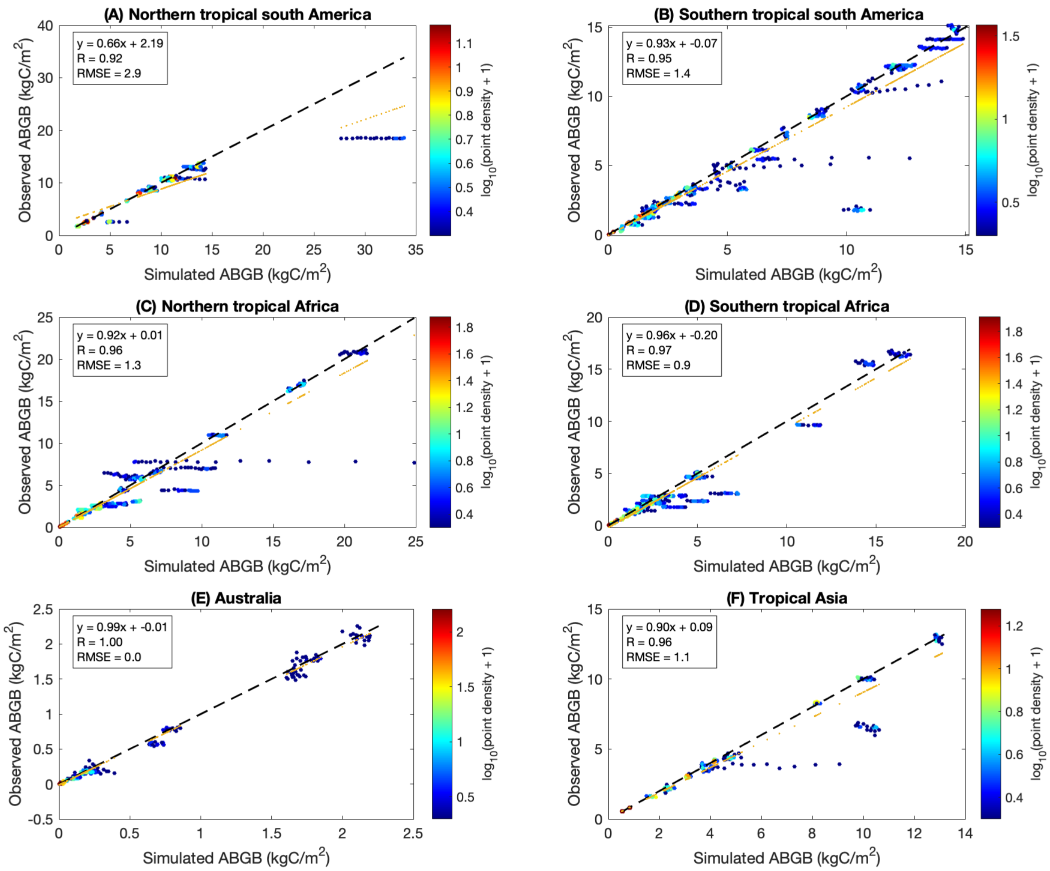

Figure S3 Heatmap of modeled above ground and below ground biomass (ABGB) compared to observations at monthly temporal resolution (2001-2021) at pixel levels (4º (latitude) x 5º (longitude)). The observations are annual, so the values within the same year are same. The pantropic region was grouped into Asia (AS), Australia (AU), Northern tropical Africa (NAF) (north of Equator), Southern tropical Africa (SAF) (south of Equator), Northern hemisphere South America (NSAM), and Southern hemisphere South America (SSAM). The R values, root mean square values, and linear fitting are labeled in each subplot. Unit: KgC/m^2.

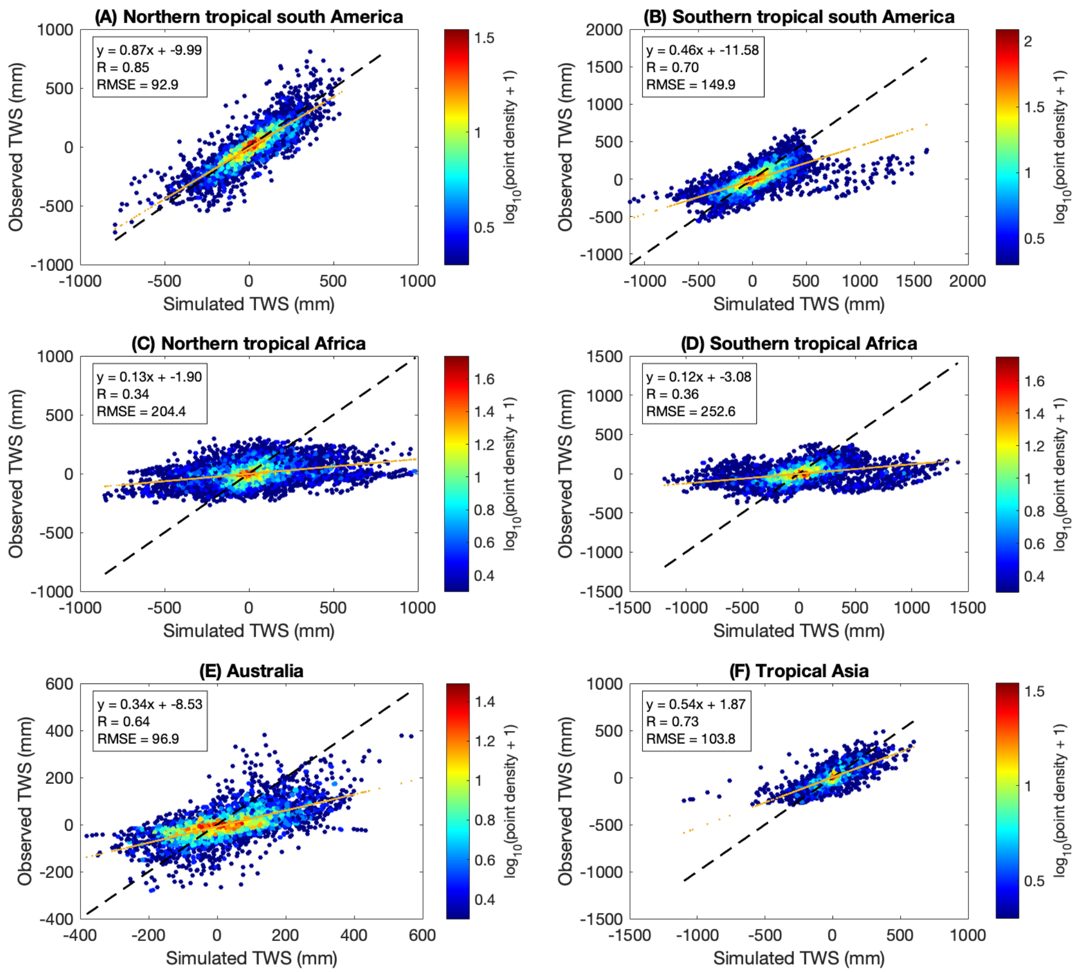

Figure S4 Heatmap of modeled total water storage (TWS) compared to observations from GRACE at monthly temporal resolution (2001-2021), at pixel levels (4º (latitude) x 5º (longitude)). The pantropic region was grouped into Asia (AS), Australia (AU), Northern tropical Africa (NAF), Southern tropical Africa (SAF), Northern hemisphere South America (NSAM), and Southern hemisphere South America (SSAM). Unit: mm.

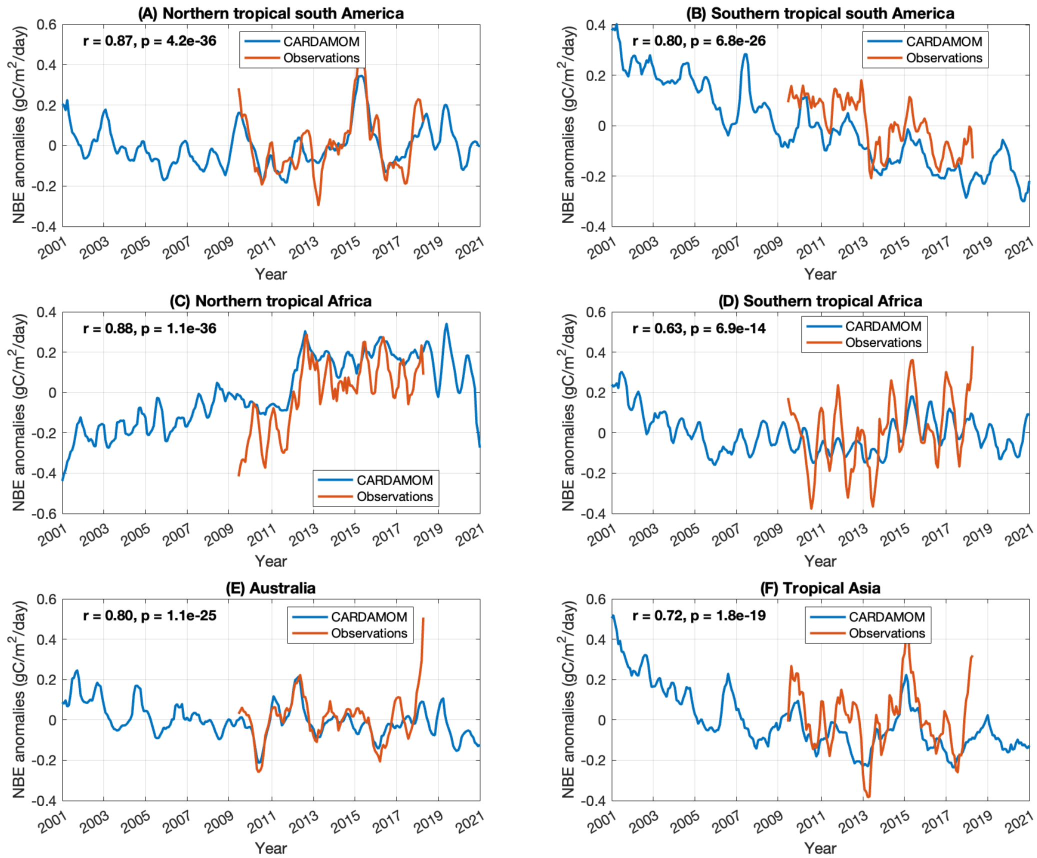

Figure S5 Modeled tropical five-month running mean of NBE anomalies compared to observations aggregated at sub-continental scale. Red lines are observations and black lines are mediums from data-model fusion posterior distribution. The pantropic region was grouped into Asia (AS), Australia (AU), Northern tropical Africa (NAF), Southern tropical Africa (SAF), Northern hemisphere South America (NSAM), and Southern hemisphere South America (SSAM). Unit: $gC/m^2/day$. The correlation and p-value are labeled in each subplot.

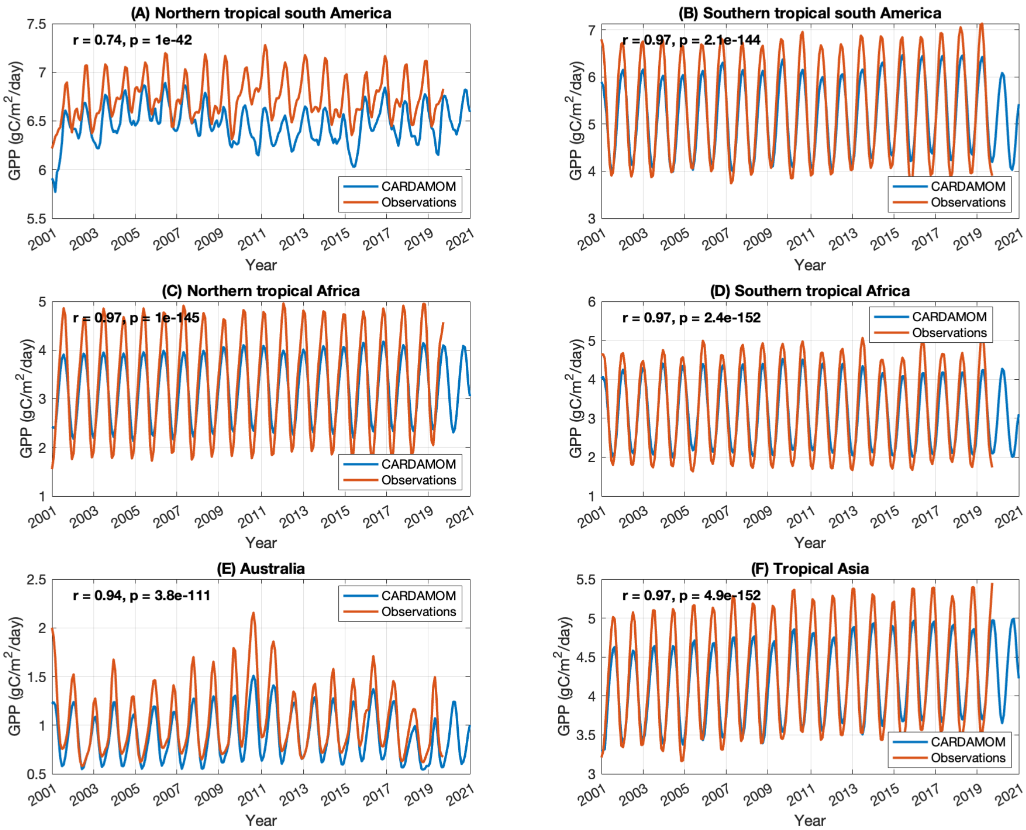

Figure S6 Modeled tropical GPP compared to observations aggregated at sub-continental scale. Red lines are observations and black lines are mediums from data-model fusion posterior distribution. The pantropic region was grouped into Asia (AS), Australia (AU), Northern tropical Africa (NAF), Southern tropical Africa (SAF), Northern hemisphere South America (NSAM), and Southern hemisphere South America (SSAM). Unit: $gC/m^2/day$. The correlation and p-value are labeled in each subplot.

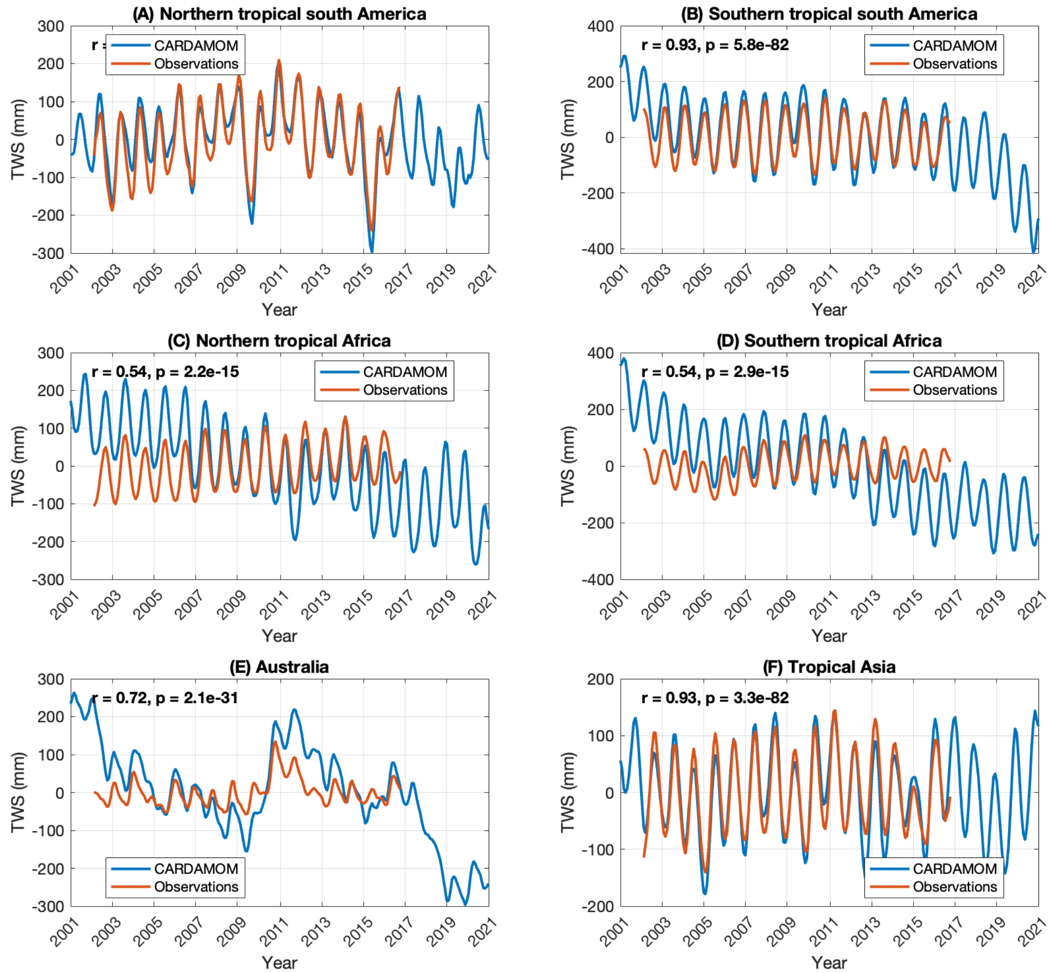

Figure S7 Modeled tropical TWS compared to observations aggregated at sub-continental scale. Red lines are observations and black lines are mediums from data-model fusion posterior distribution. The pantropic region was grouped into Asia (AS), Australia (AU), Northern tropical Africa (NAF), Southern tropical Africa (SAF), Northern hemisphere South America (NSAM), and Southern hemisphere South America (SSAM). Unit: mm. The correlation and p-value are labeled in each subplot.

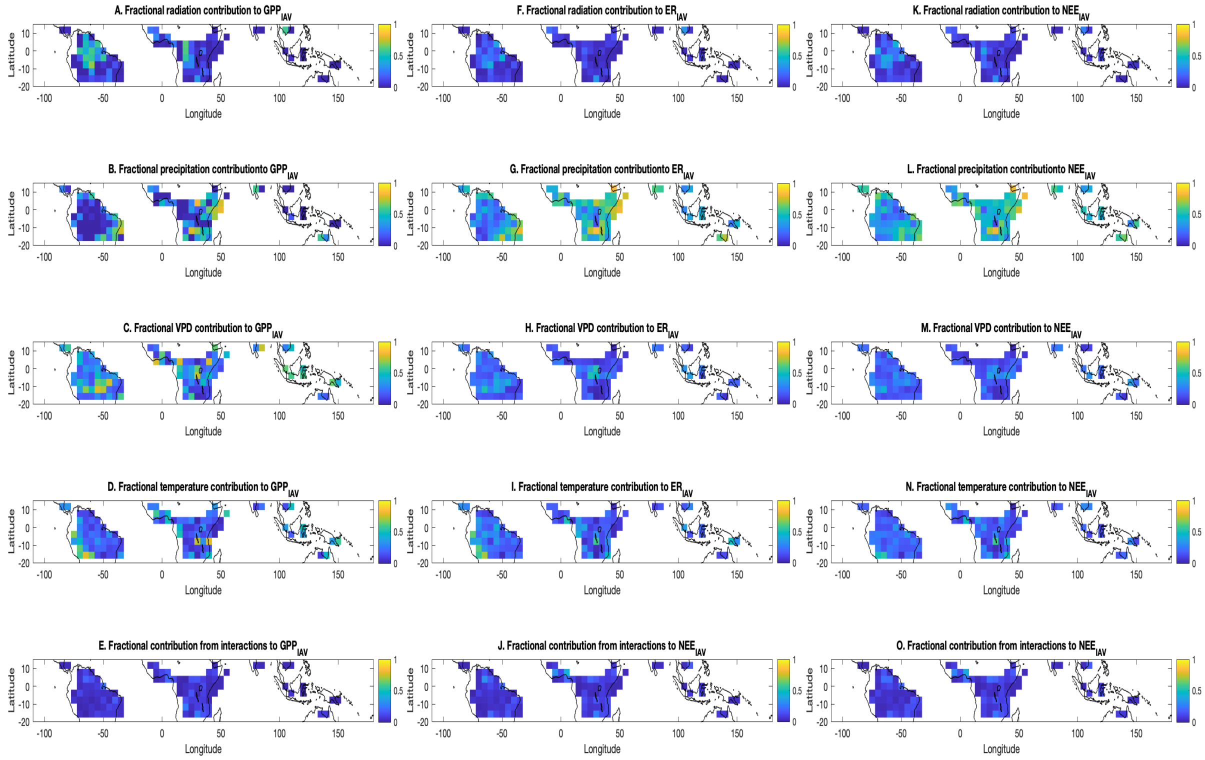

Figure S8. Fractional contributions of radiation, precipitation, VPD, temperature, and their interactions to GPP_{IAV} (A-E), ER_{IAV} (F-J) and NEE_{IAV} (K-O).

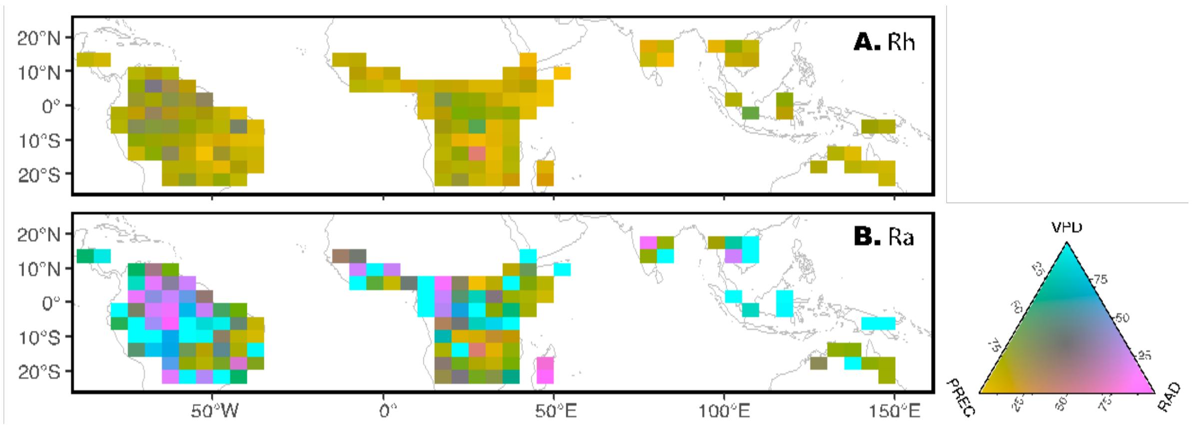

Figure S9. Maps showing the dominant climate factors for heterotrophic respiration (Rh) and Autotrophic respiration (Ra) during 2010-2021. The three largest climate factors for carbon fluxes IAV, precipitation, VPD, and radiation, are chosen to calculate their relative importance in this tricolored map.

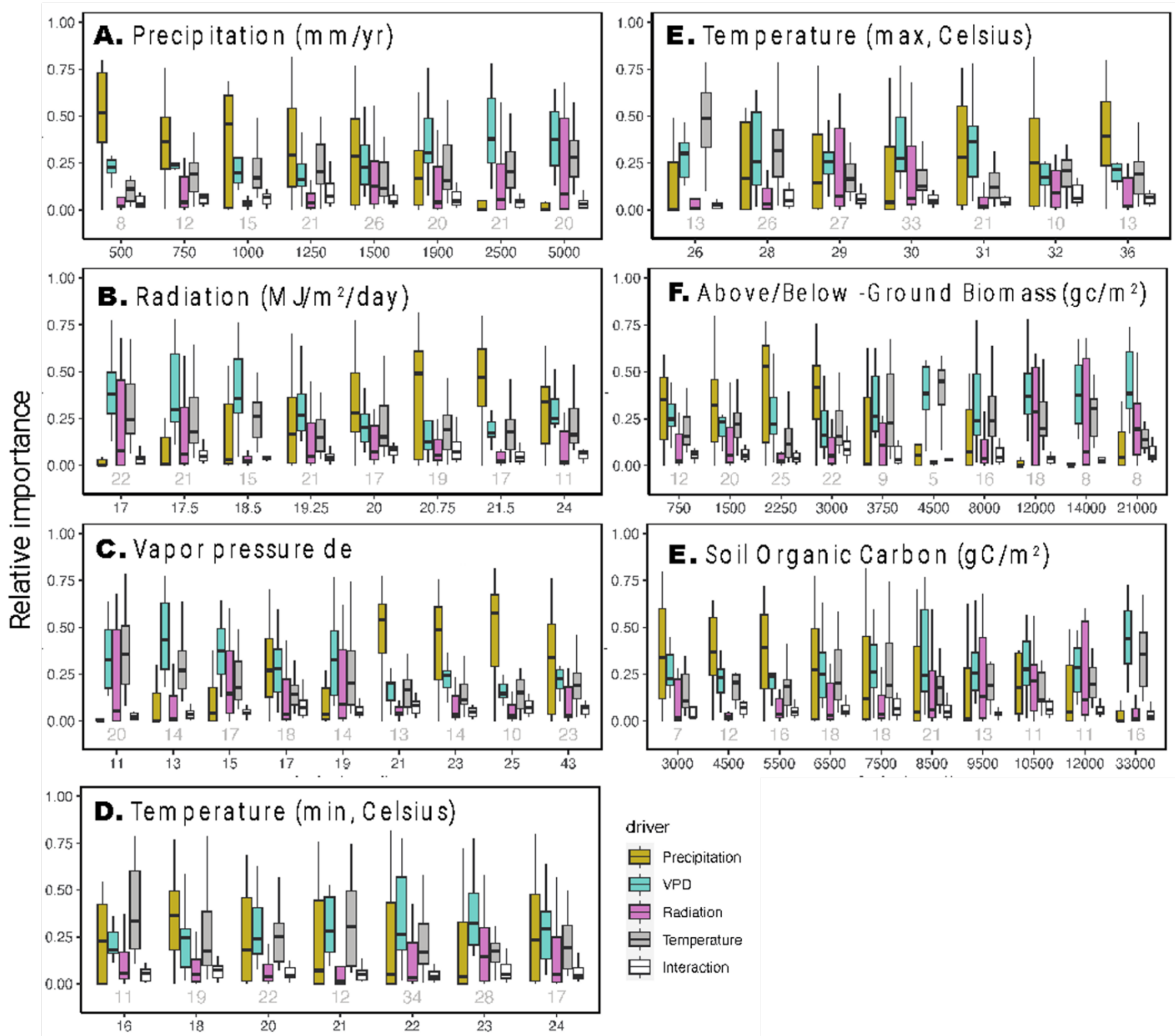

Figure S10. Relative importance of climate drivers on GPP_{IAV} per category of pixels grouped by environmental and biological mean states. Grey numbers on the bottoms are the count of pixels that falls in each category shown in the x axis.

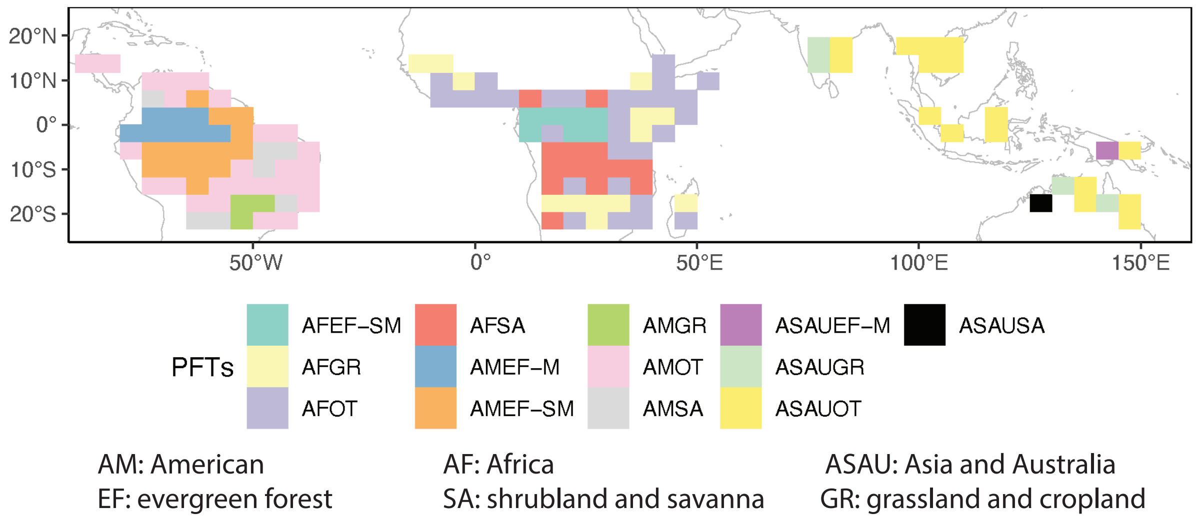

Figure S11 Vegetation map according to MODIS MCD12C v6.1. AF is tropical Africa. AM: American, AF: Africa, ASAU: Asia and Australia. EF: evergreen forest, SA: semi-arid (shrubland and savanna), GR: grassland and cropland, OTther (none of those PFTs have larger than 60% of areal coverage). Rainforest is divided into two categories using MAP=2800mm as threshold (MAP>2800mm for Moist rainforest and MAP<2800mm for Seasonally Moist rainforest (SM)).

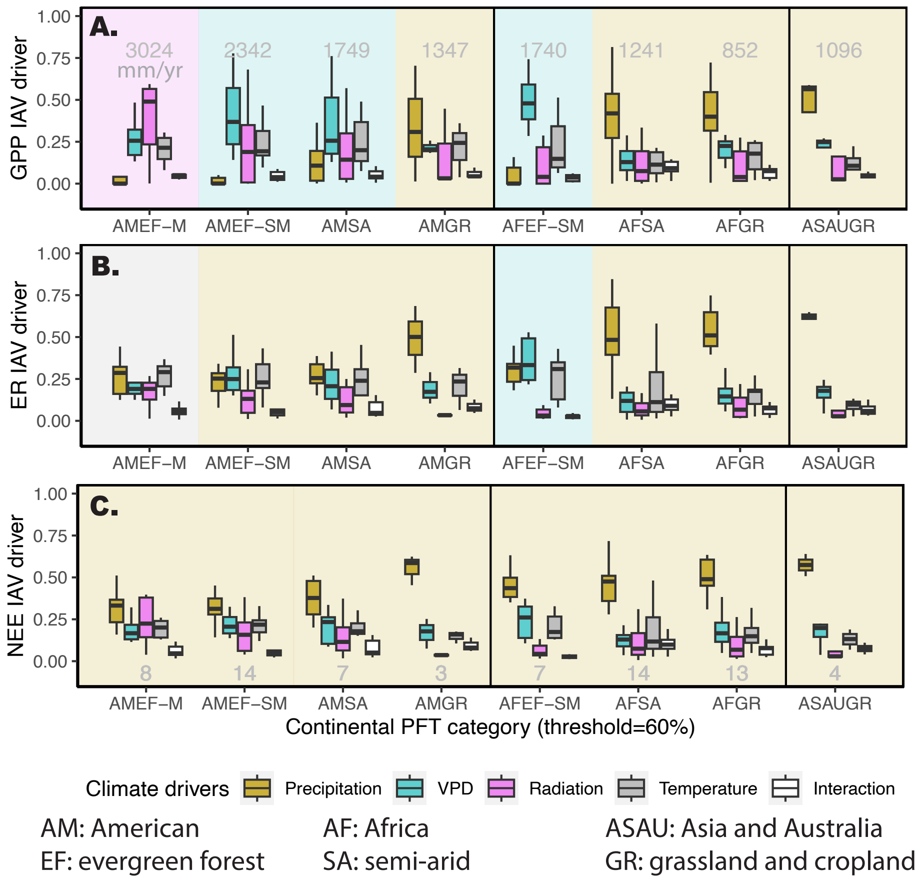

Figure S12. The relative contributions of climate factors to the IAV of GPP, ER, and NEE during 2010-2021. Grid-cell data is grouped according to the continent and the main plant functional types (PFTs, using land cover data from MODIS (Figure S11), threshold=60%). AM: American, AF: Africa, ASAU: Asia and Australia. EF: evergreen forest, SA: shrubland and savanna, GR: grassland and cropland. Rainforest is divided into two categories using MAP=2800mm as threshold (MAP>2800mm for Moist rainforest and MAP<2800mm for Seasonally Moist rainforest). Boxes and whiskers show median, 5%, 25%, 75%, and 95% percentiles from pixels that fall in the same continental and PFT category. The gray numbers on the top are the average MAP from all the pixels. The gray numbers on the bottom are the number of 4° (latitude) x 5° (longitude) pixels that are covered by the same PFT for each continent.

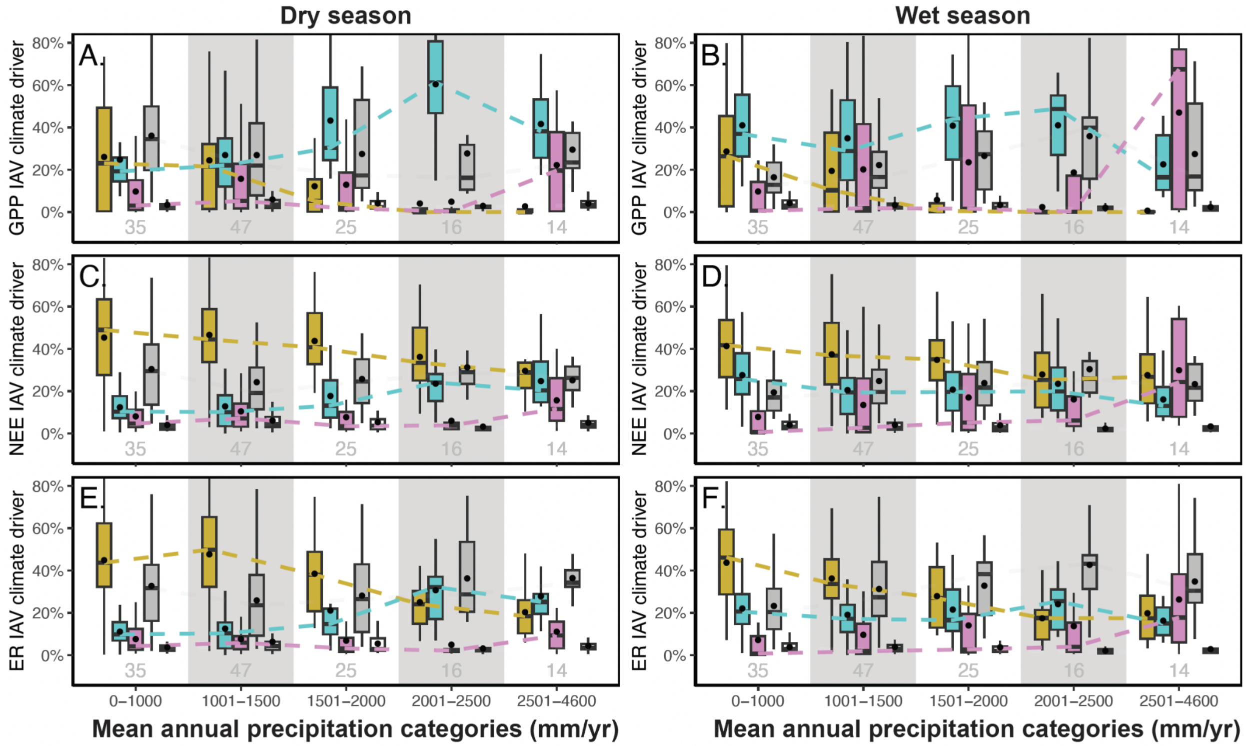

Figure S13. Relative importance of climate drivers to the IAV of GPP, ER, and NEE during 2010-2021 in the dry/wet season. Grid-cell data is grouped according to the Mean Annual Precipitation (MAP), boxes and whiskers show median, 5%, 25%, 75%, and 95% percentiles from pixels that fall in the same MAP category, points are the mean values. The gray numbers on the bottom are the number of 4º (latitude) x 5º (longitude) within each MAP category.

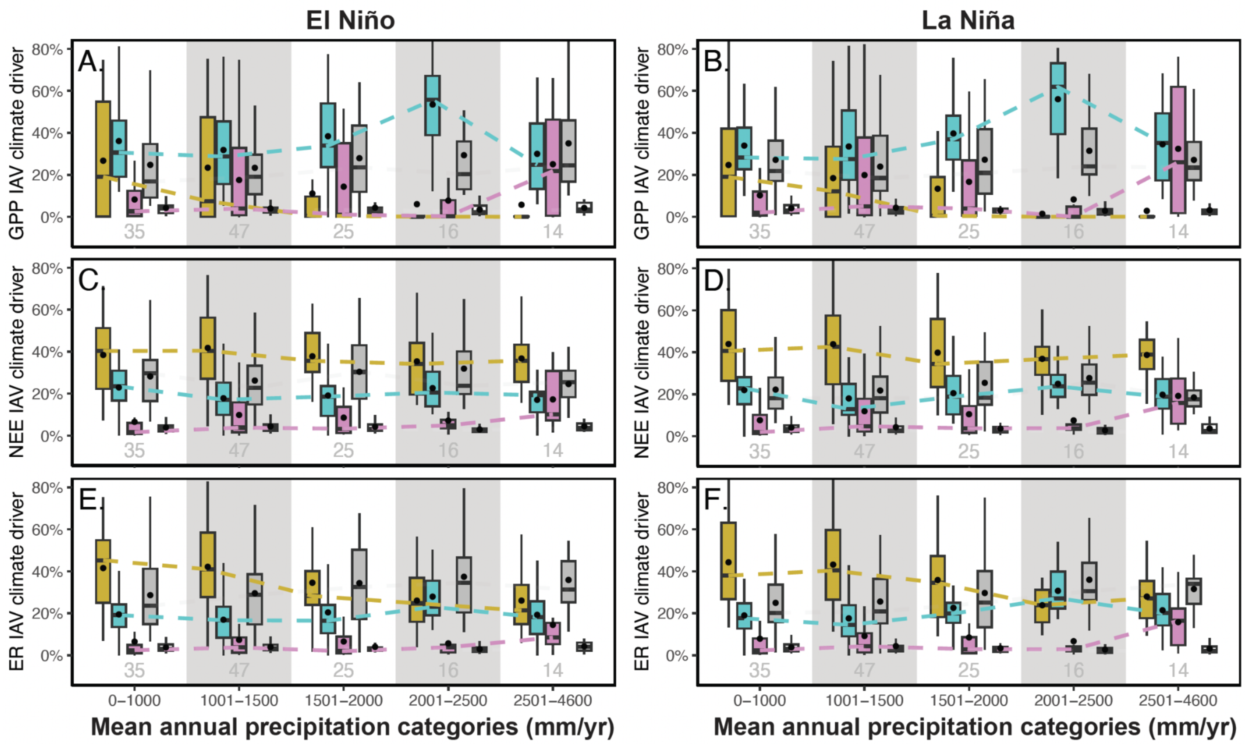

Figure S14. Relative importance of climate drivers to the IAV of GPP, ER, and NEE during 2015-2016 El Niño and 2010-2011 La Niña. Grid-cell data is grouped according to the Mean Annual Precipitation (MAP), boxes and whiskers show median, 5%, 25%, 75%, and 95% percentiles from pixels that fall in the same MAP category, points are the mean values. The gray numbers on the bottom are the number of 4º (latitude) x 5º (longitude) within each MAP category.

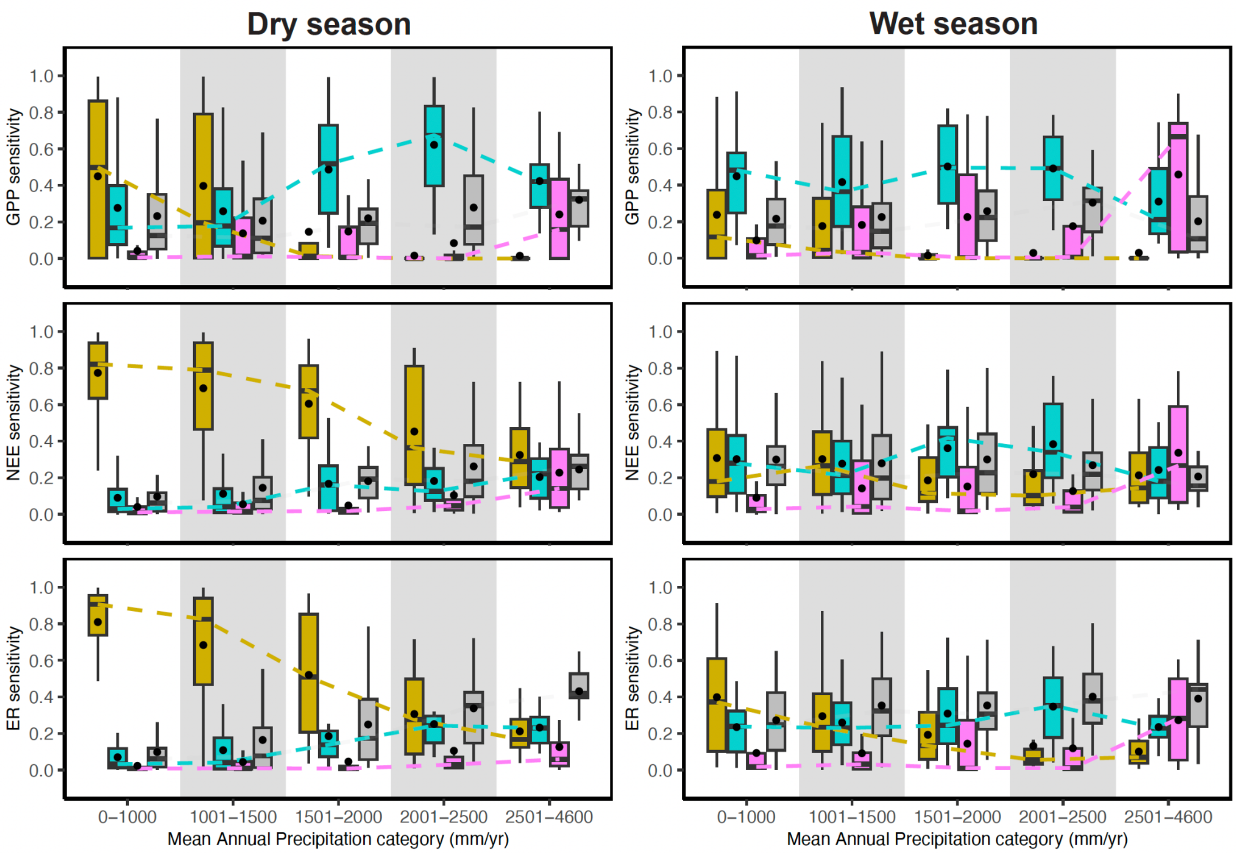

Figure S15. Sensitivity of GPP, ER, and NEE to climate drivers in the dry and wet seasons of 2010-2021. Grid-cell data is grouped according to the Mean Annual Precipitation (MAP), boxes and whiskers show median, 5%, 25%, 75%, and 95% percentiles from pixels that fall in the same MAP category, points are the mean values. The gray numbers on the bottom are the number of 4º (latitude) x 5º (longitude) within each MAP category.

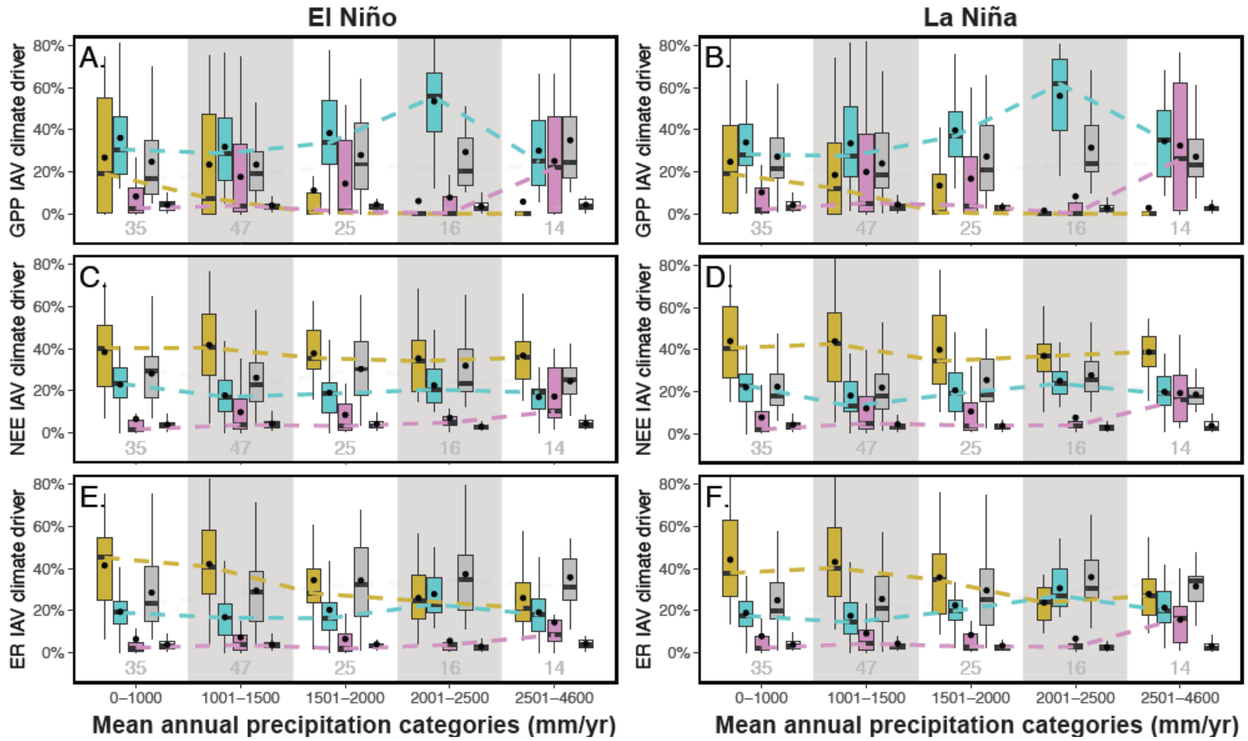

Figure S16. Sensitivity of GPP, ER, and NEE to climate drivers during 2015-2016 El Nino and 2010-2011 La Nina. Grid-cell data is grouped according to the Mean Annual Precipitation (MAP), boxes and whiskers show median, 5%, 25%, 75%, and 95% percentiles from pixels that fall in the same MAP category, points are the mean values. The gray numbers on the bottom are the number of 4º (latitude) x 5º (longitude) within each MAP category.

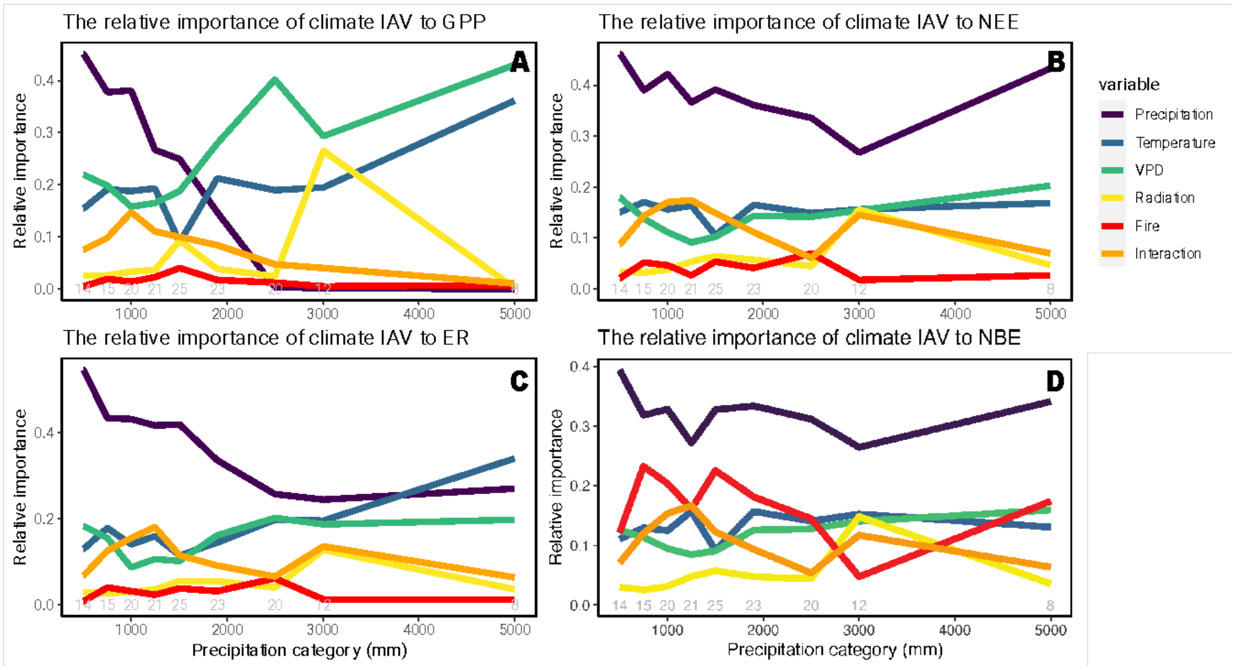

Figure S17. The relative importance of fire and interactions among fire, radiation, temperature, VPD is small to GPP, ER, and NEE IAV. Grey numbers on the bottom are counts of pixels that falls in each precipitation category.

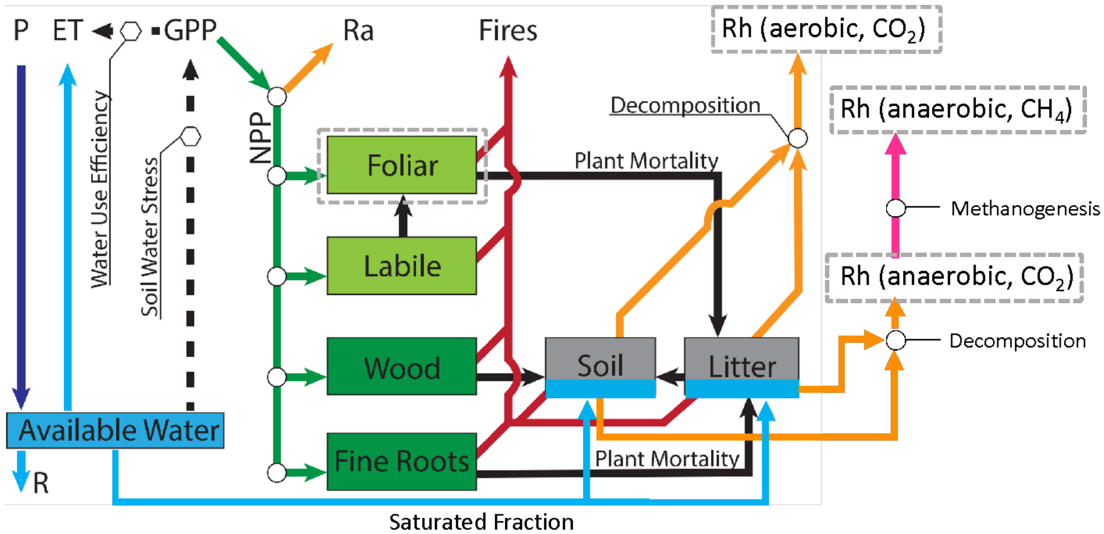

Figure S18. Diagram of DALEC, adapted from Quetin et al., 2020; Bloom et al. 2016. P is precipitation, ET is evapotranspiration, R is runoff, GPP is gross primary production of CO_2, Ra is autotrophic respiration, and Rh is heterotrophic respiration.

Table S1.

	Precipitation	Temperature	VPD	Radiation
Scenario 1 (control run)	- *	-	-	-
Scenario 2 (perturbed run)	Climatology **	-	-	-
Scenario 3 (perturbed run)	-	Climatology	-	-
Scenario 4 (perturbed run)	-	-	Climatology	
Scenario 5 (perturbed run)	-	-	-	Climatology

Table S1. Scenarios of control and perturbed model runs.
* - indicate using original climate data from ERA5
** Climatology indicate swapping the original climate data from ERA5 with the climatology mean. eg. averaging precipitation of all the Januarys from 2010-2021 and use that value for Januarys in the perturbed run.